Opto-Electronic Advances

CN 51-1781/TN ISSN (Print) 2096-4579 ISSN (Online) 2097-3993

Spatiotemporal beam stirring in a multicore fiber

Alena Y. Kolesnikova*, Mikhail D. Gervaziev, Nikita V. Bochkarev, Denis S. Kharenko, Evgeniy V. Podivilov and Sergey A. Babin*

Citation: Kolesnikova AY, Gervaziev MD, Bochkarev NV et al. Spatiotemporal beam stirring in a multicore fiber. *Opto-Electron Adv* **9**, 260036 (2026).

https://doi.org/10.29026/oea.2026.260036

Received: 9 February 2026; Accepted: 29 May 2026; Published online: 22 June 2026

Related articles

Seeing at a distance with multicore fibers

Haogong Feng, Xi Chen, Runze Zhu, et al

Opto-Electronic Advances 2024, **7**(7): 230202 doi: 10.29026/oea.2024.230202

Advances in femtosecond laser direct writing of fiber Bragg gratings in multicore fibers: technology, sensor and laser applications

Alexey Wolf, Alexander Dostovalov, Kirill Bronnikov, et al

Opto-Electronic Advances 2022, **5**(4): 210055 doi: 10.29026/oea.2022.210055

Distributed multicore fiber sensors

Zhiyong Zhao, Ming Tang, Chao Lu

Opto-Electronic Advances 2020, **3**(2): 190024 doi: 10.29026/oea.2020.190024

More related articles in Opto-Electronic Journals Group website

Opto-Electronic Journals Group

https://www.oejournal.org

OE_Journal

@OptoElectronAdv

OEA | Opto-Electronic Advances

Article

September 2026, Vol. 9, No. 9

Open Access

Spatiotemporal beam stirring in a multicore fiber

Alena Y. Kolesnikova[1,2*†], Mikhail D. Gervaziev[1,2†], Nikita V. Bochkarev[1,2], Denis S. Kharenko[1,2], Evgeniy V. Podivilov[1,2] and Sergey A. Babin[1,2*]

Abstract: Multicore fibers (MCFs) are perspective for telecommunications, sensing, imaging, and laser technologies. Here, the effect of spatiotemporal beam stirring between weakly coupled cores is observed for sub-nanosecond narrowband pulses of several kW peak power propagating in ~10 m long 7-core fiber, for the first time to our knowledge. In contrast to the low-power domain where the output power distribution in the cores is random with large fluctuations sensitive to fiber disturbances, at high power of the input pulse injected in the central core the output power becomes equalized between the cores with fluctuations reduced to <5% being insensitive to disturbances. Similar behavior is observed in cut-back experiments showing that equi-partition is approached at a distance of ~5 m. The performed modeling describes well the experimental results and clarifies mechanisms of the new effect caused by a large nonlinear phase shift changing along the pulse and thereby resulting in statistical averaging over the pulse length of multidirectional power transfer processes between cores, thus leading to the robust equilibrium (equi-partitition for hexagonal MCF topology). At the same time, the combined output beam measured in a far field takes a stable bell-shaped profile instead of speckled beam at low powers, similar to the beam self-cleaning effect in multimode fibers.

Keywords: multicore fiber; Kerr nonlinearity; beam stirring

DOI: 10.29026/oea.2026.260036 | CSTR: 32247.14.oea.2026.260036

Citation: Kolesnikova AY, Gervaziev MD, Bochkarev NV et al. Spatiotemporal beam stirring in a multicore fiber. *Opto-Electron Adv* **9**, 260036 (2026).

1 Introduction

Multicore fibers (MCFs) were initially proposed and implemented as one of the possible methods of spatial division multiplexing (SDM) for high-capacity optical communications, which may overcome the limitations of a conventional singlemode fiber (SMF)[1]. The MCF-based SDM technology is treated as much more cost- and power-efficient in comparison with parallel deployment of multiple SMFs and may be less affected by a cross-talk between parallel spatial channels in comparison with multimode fibers where significant overlap between transverse modes is always present. The potential of MCF-based SDM technology has recently been confirmed by experimental demonstration of >10 Pb/s transmission[2].

At the same time, MCFs are considered as promising means of generating, amplifying, and delivering high power/energy continuous wave (CW)/pulsed radiation[3] as well as a favorable medium for new types of fiber sensors[4], which overcome limitations of conventional singlemode fibers. Implementation of FBG arrays inscribed in MCFs by femtosecond laser pulses with high spatial resolution over transverse and longitudinal coordinates[5] offers new opportunities in 3D shape sensing, as well as in new designs of fiber laser cavities. The selective inscription of FBGs with individual parameters in different cores allows to control spatio-spectral characteristics of output beam in CW fiber lasers based on MCFs. The individual cores may generate either independently delivering multiple uncoupled beams at different wavelengths defined by individual FBGs or generate coupled beams in coupled-core MCF at single wavelength corresponding to the maximum of geometric-mean reflection of individual FBGs[6]. At the same time, the closely spaced coupled cores may have large mode area

Received: 9 February 2026

Accepted: 29 May 2026

Published online: 22 June 2026

[1]Institute of Automation and Electrometry SB RAS, Novosibirsk 630090, Russia; [2]Novosibirsk State University, Novosibirsk 630090, Russia.

[†]These authors contributed equally to this work.

*Correspondence: AY Kolesnikova, E-mail: a.kolesnikova@g.nsu.ru; SA Babin, E-mail: babin@iae.nsk.su

(LMA) that offers enhanced power scaling of CW lasers at the intensity kept at rather low level thus reducing the role of nonlinear effects such as Kerr-nonlinearity induced spectral broadening, whereas the predominantly generated in-phase supermode may be coherently combined into a nearly diffraction limited beam[7].

MCFs are also used for power scaling of short-pulse laser systems[8] being a more reliable alternative to a rather complicated and expensive spatially separated fiber amplifiers with coherently combined output which already outperform single-emitter systems[9]. The implementation of active MCFs using a single-beam seed divided among independent amplifying LMA cores and a subsequent coherent combining of output beams with active control of their phases enables a kW-level average power of ultrashort pulse trains[8]. At the same time, in coupled-core MCFs close arrangement of multiple doped cores in a shared cladding results in either internal self-organization or external formation of supermodes being kept unchanged over long fiber lengths and resistant to nonlinear effects. In this way, an efficient out-of-phase (with π-phase shift in neighbor cores) supermode amplification of short pulses in a circular 6-core Yb-doped fiber[10] or in a MCF with square $N\times N$ array of coupled cores[11] is shown to be resistant to discrete modulation instability induced by Kerr nonlinearity and can carry total power greatly exceeding the self-focusing threshold for single-core fiber.

The nonlinear effect of self-focusing manifests itself in MCFs as a light localization within a few (or even single) cores accompanied by a pulse length compression at increasing energy[12]. The numerical simulation predicts nonlinear combining into a single core of ~90% of the total energy of pulses initially injected into all cores of a hexagonal 7-core MCF and a pulse compression factor of about 720 in a 19-core ring MCF. Such pulse localization/compression in the central core of a hexagonal 7-core fiber was experimentally observed for sub-μJ 370 fs pulses compressed to 53 fs with corresponding peak power increase >2 MW[13]. An opposite nonlinear effect has recently been observed in a strongly coupled multicore waveguide arrangements in bulk silica[14] where sub-MW pulsed beam initially coupled to one of the cores is redistributed between the cores so that up to 78% of the transmitted power becomes concentrated in a fundamental mode of the multicore system (supermode with the highest propagation constant) with increasing input peak power/nonlinearity. The effect is explained in terms of all-optical thermodynamic phenomena, namely Joule–Thomson expansion process mediated by photon–photon interactions whereby the temperature of the optical gas drops to nearly zero tending the system to ground state.

Here we numerically and experimentally demonstrate, for the first time to our knowledge, another nonlinear effect in a hexagonal 7-core MCF as an example, which manifests itself at pulse propagation with much lower peak powers corresponding to weak nonlinearity, far from the self-focusing threshold. In the presence of weak random (linear) coupling between the cores (e.g. at fiber coiling) the pulse becomes randomly redistributed between the cores (regardless of the initial conditions) with 100% fluctuations of power in individual cores as the pulse propagates along the fiber. It is revealed that at kW-level peak power, the fluctuations greatly reduce at the pulse propagation over tens meters of MCF so that the power in the individual cores is exactly equalized and stabilized becoming resistant to external disturbances of the fiber, in contrast to the case of linear random coupling. The dependence of the nonlinear stabilization length on the pulse peak power and the coupling strength of MCF cores, as well as the amplitude and characteristic length of the refractive index fluctuations in the cores is studied numerically and compared with experiment. Following the results of the numerical and experimental investigations, qualitative explanation of this new effect based on spatio-temporal beam stirring within individual pulse is provided.

2 Experiment

In our experiments, we launched the beam from the narrow-band Q-switched microchip laser Standa STA-01-7-OEM (central wavelength $\lambda = 1064$ nm, pulse duration 435 ps, repetition rate 1 kHz) into the passive 7-core fiber (7CF) produced by FORC RAS (see ref.[5] for details). At the wavelength of 1064 nm each core of 7CF acts similarly to a single-mode fiber with the mode field diameter of 6.4 μm, the distance between cores is 17.3 μm. A schematic of the setup is demonstrated in Fig. 1. In this system, the transmission reached 55% while the laser beam is optimally focused in a core. The beam waist diameter was fitted to the mode field

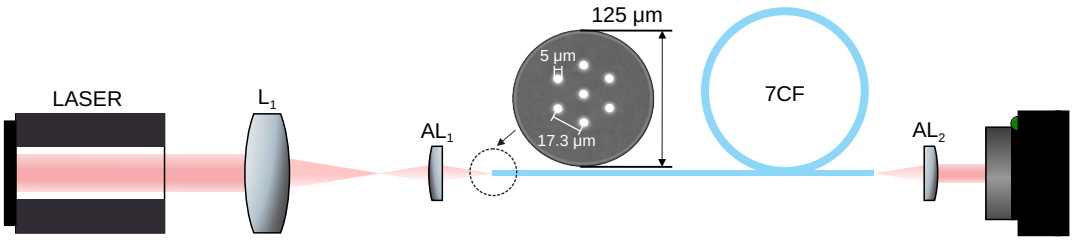


Fig. 1 | Experimental setup: L_1 – lens, $AL_{1,2}$ – aspheric lenses for beam collimation at the input and output of the 7CF, the image of the fiber output beam is captured with CMOS camera.

diameter of each core. The output power distribution between the cores was recorded using a Gentec Beamage-4M beam profiler. To minimize/average the influence on the studied spatial dynamics of refractive index fluctuations along a core, an 11 m long piece of fiber was coiled into a ring with a diameter of 6 cm.

The obtained experimental data were used to plot the output power distribution in the cores as a function of the input pulse peak power (P_{in}), taking transmission into account (Fig. 2(a)). For this purpose, we wrote a Python script that processes a near-field profile image captured by the camera. It sums the intensity at the $1/e^2$ level for each beam, resulting in a relative power distribution. At relatively low peak power ($P_{in} = 0.13$ kW), the beam initially injected into the central core is randomly redistributed between all the cores. As we increase the input peak power, the observed power deviations in the cores start to reduce, reaching an almost complete equalization (with fraction value of ~14% for all cores) at $P_{in} = 6.32$ kW which corresponds to the average pulse-train power of ~2.75 mW. We did not observe significant changes in the input/output power transmission ratio between the low- and the high-power excitation regimes, which indicates that the effect does not arise due to a change in the linear losses. To demonstrate the nonlinear nature of the equalization effect, we plotted the difference between the maximum and minimum output power fraction in the cores as a function of the input peak power (Fig. 2(b)). As we increased the input peak power, the measured spread of the output power fractions dropped down from >30% to <5%. This key experimental dependence illustrating the new nonlinear effect of beam stirring in MCFs is used for further comparison with the results of analytical and numerical modeling described below.

In addition, by measuring optical spectra with the use of a Yokogawa AQ6370D analyzer, we revealed that the spatial effect is accompanied by the slight broadening of the narrowband optical spectra beyond the resolution of spectrum analyzer because of self-phase modulation. It should be noted that at the maximum power a shifted Raman scattering peak becomes visible, but the equi-distribution is already formed at lower powers.

For a deeper insight into the nonlinear dynamics of the beam propagating in 7CF with randomly coupled cores, we performed a study of beam evolution along the fiber by its gradually backward cutting at the injection conditions unchanged. The relative power difference in the cores starting from the input face (corresponding to the launch into the central core) up to 11 meters length is demonstrated in Fig. 3 for two different levels of P_{in}. Over the first two meters, the beam undergoes a similar evolution, showing a decrease in the spread between the core fractions. However, the dynamics diverge significantly at longer distances. At low power, the spread between the core fraction difference fluctuates around 30% and does not reach equal powers. For higher input powers, the difference continues to decrease. At that the equi-partition emerges at different length depending on power, so that at the maximum length of 11 m the difference decreases with increasing power as shown in Fig. 2(b).

Finally, we studied the evolution of transverse beam profiles at the 11-m MCF output. We captured the near field (NF) and – using the Fourier lens – far field (FF) images (Fig. 4). At low power (Fig. 4(a)), the NF power distribution between cores is random and unstable, with the maximum in one of the cores, whereas some other ones almost have no power in them. At high power (Fig. 4(c)) equi-partition was established, and all the cores have nearly equal output power. At the same time, FF images demonstrate noticeable dynamics during the transition from linear regime to nonlinear one. It is noteworthy that at low power (Fig. 4(d)), such a beam has a speckled structure, but at high power the

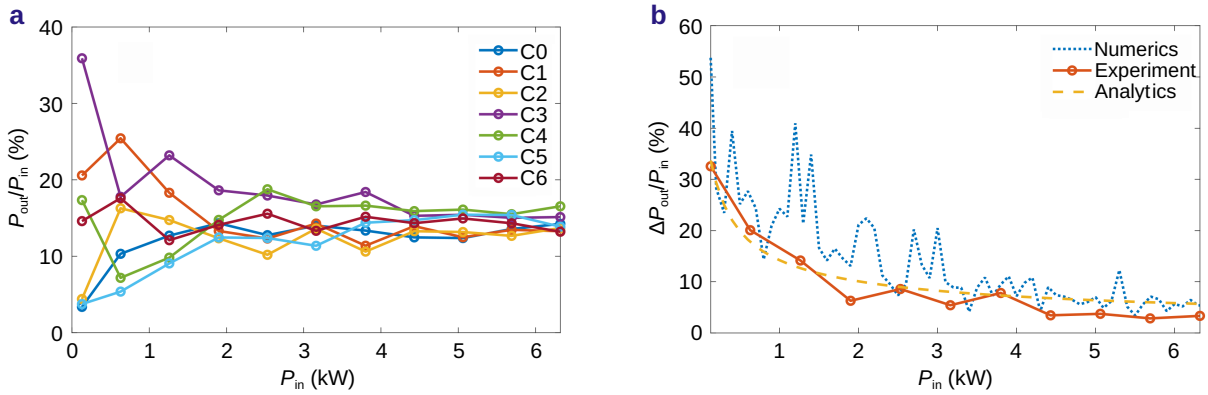


Fig. 2 | (a) The output power fraction in individual cores (C0-C6, C0 is central) as a function of the input peak power of the pulse propagating in a 11-m 7CF coiled into a ring with diameter of 6 cm. (b) The relative difference between the maximum and minimum output power (core fractions) as a function of the input peak power (orange line corresponds to experimental data, blue line – to numerical modelling, yellow line – to analytical approximation).

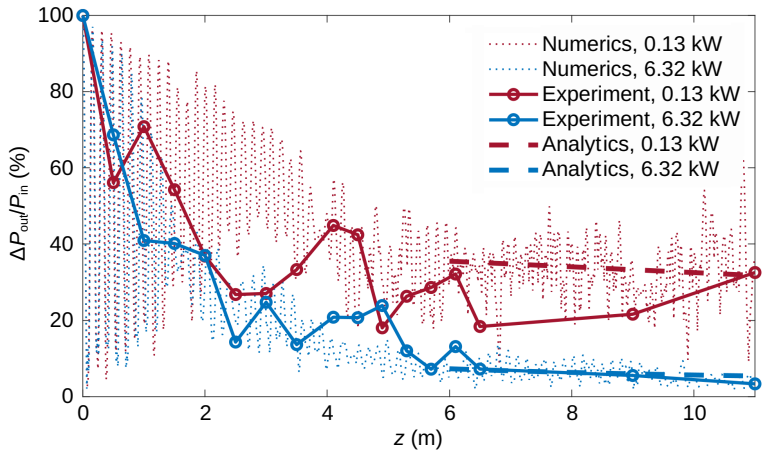


Fig. 3 | The relative difference between the maximum and minimum power (core fractions) versus fiber length for two input peak power values.

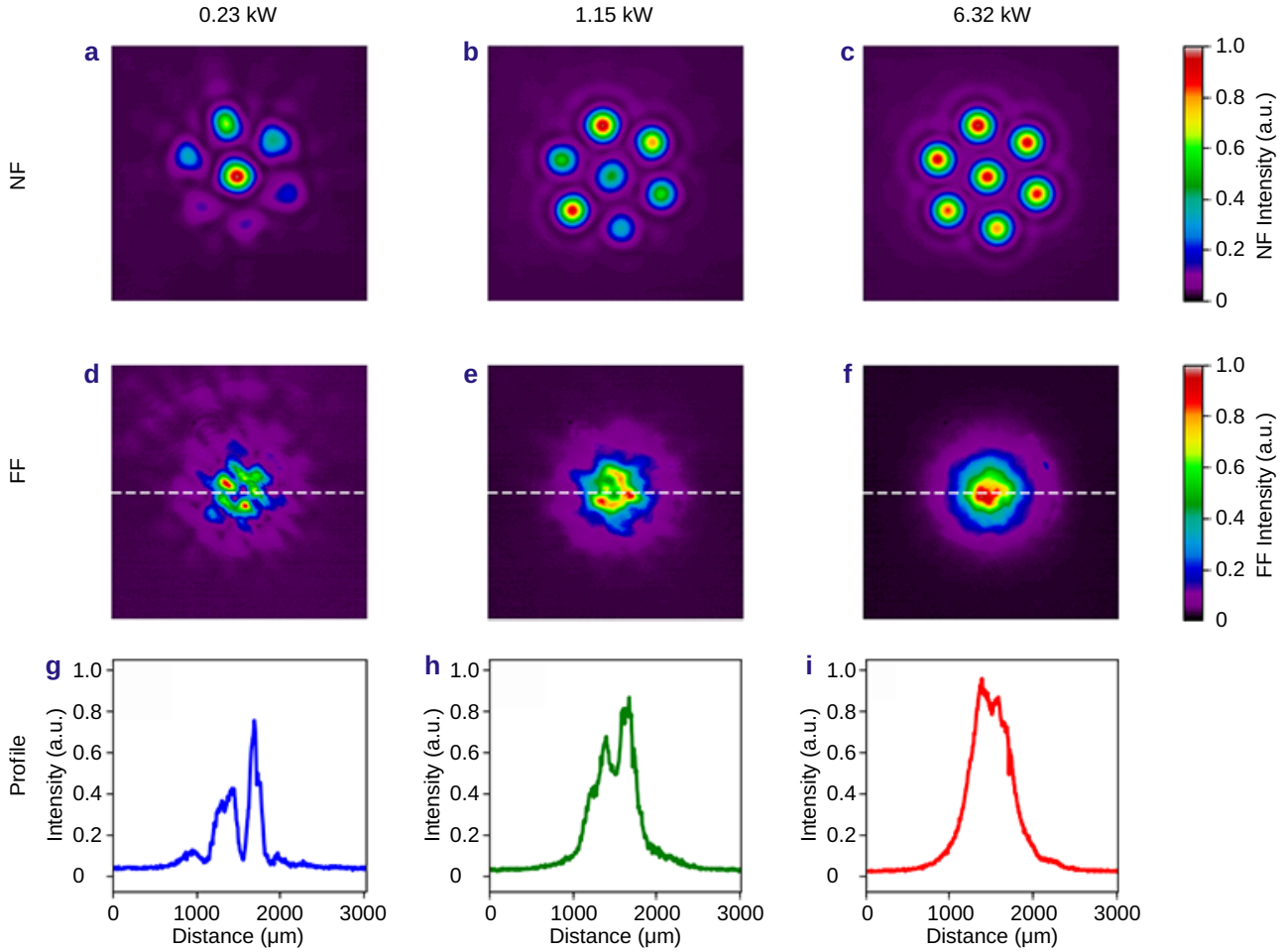


Fig. 4 | NF images of the 7CF output captured at 1064 nm (a–c) demonstrate the spatial beam stirring, namely the formation of 7 beams with equal intensities when the P_{in} increases. FF images (d–f) demonstrate the transition from speckled structure to the bell-shaped transverse profile (g–i). Fiber length - 11 m. The images were taken in different time than the data shown in Fig. 2(a), therefore unstable distribution between cores at low power does not correspond to that in Fig. 2(a).

beam acquires a characteristic bell-shaped profile with enhanced brightness and quality (Fig. 4(f)), which may be result of statistical averaging or partial coherence between the cores. This dynamic resembles another notable spatial nonlinear effect, namely spatial Kerr self-cleaning, which occurs in multimode fibers[15]. In addition, we investigated the stability of the output spatial dynamics against external localized mechanical stress. At low powers, external disturbances applied to the fiber significantly altered the FF speckle structure, as well as the NF intensity distribution between the cores (see the video files "NF_Low_Power" and "FF_Low_Power" in the supplementary information). At high powers, the beam stirring is a robust effect that being insensitive to disturbances such as bending and twisting (see the video files "NF_High_Power" and "FF_High_Power" in the supplementary information) which reinforces the similarity with Kerr beam self-cleaning. This analogy requires a deeper understanding of key physical mechanisms of the effect that can be achieved by the development of the appropriate model.

3 Modelling and comparison with experiment

The pulse propagation model in a multicore fiber can be written as follows. The electric field is the sum of the pulses propagating in the cores $E=\sum_{j=0}^{6}A_j(z,t)\boldsymbol{\Psi}(\boldsymbol{r}-\boldsymbol{r}_j)\mathrm{e}^{\mathrm{i}\omega t-\mathrm{i}kz}$ with the carrier frequency $\omega=281$ THz (λ=1064 nm) and the propagation constant $k=(2\pi n_{\mathrm{eff}})/\lambda=8.6$ μm^{-1}, where n_{eff} is the average effective refractive index in the cores. Here $\boldsymbol{\Psi}(\boldsymbol{r}-\boldsymbol{r}_j)$ is the normalized spatial distribution of core j fundamental mode in fiber cross-section, $\boldsymbol{r}_j$ is the coordinate of core j center ($j=0,\cdots,6$). The strength of the coupling between the modes of different cores is determined by the overlap integral $J\sim\int(n_2-n_1)/n_1\boldsymbol{\Psi}(\boldsymbol{r}-\boldsymbol{r}_j)\boldsymbol{\Psi}(\boldsymbol{r}-\boldsymbol{r}_k)\mathrm{d}^2r(\forall j\neq k)$, the non-zero value of which is due to the overlap of the exponentially decaying tails of the core mode with neighboring modes, and its propagation evolution is described by a system of coupled equations:

$$\begin{cases}\dfrac{\mathrm{d}A_0}{\mathrm{d}z}=\mathrm{i}\delta n_0(z)kA_0+\mathrm{i}\left(k+\dfrac{\mathrm{i}n_{\mathrm{eff}}}{c}\dfrac{\mathrm{d}}{\mathrm{d}t}\right)J\sum_{j=1}^{6}A_j \\ \qquad\qquad +\mathrm{i}\gamma|A_0|^2A_0 \\ \dfrac{\mathrm{d}A_j}{\mathrm{d}z}=\mathrm{i}\delta n_j(z)kA_j+\mathrm{i}\left(k+\dfrac{\mathrm{i}n_{\mathrm{eff}}}{c}\dfrac{\mathrm{d}}{\mathrm{d}t}\right)J(A_0+A_{j-1} \\ \qquad\qquad +A_{j+1})+\mathrm{i}\gamma|A_j|^2A_j\end{cases}, \quad (1)$$

here the square of the field amplitude is normalized to the power. The coefficient of self-phase modulation due to Kerr nonlinearity is $\gamma=5\times10^{-3}(\mathrm{W}\cdot\mathrm{m})^{-1}$ in each core, which corresponds to the fused silica core with the mode field diameter of $\sim$ 6.4 μm. The addition of a time derivative in the linear coupling term is necessary to account for the different group velocities. The model includes the relative difference in refractive indices $\delta n_j(z)$ in the cores arising at fiber fabrication and its winding on a spool. Direct measurement of the variation of the refractive index is not experimentally feasible and can only be estimated indirectly from the dynamics of radiation propagation. So, it is randomly varied such that $\sum_{j=0}^{6}\delta n_j=0$ and does not exceed a certain specified value $|\delta n_j|<\delta n_{\max}$. The initial state is the pulse injected to the central core at the input $A_0(0,t)=\sqrt{P_{\mathrm{in}}}/\cosh(t/\tau)$, where τ is a pulse duration, P_{in} is a peak input power.

The numerical scheme for solving the system of Eq. (1) is based on the Split-Step method, where the linear and nonlinear parts of the equation are calculated independently; the linear part is calculated using the matrix exponent. To calculate the time derivative in a step with a linear coupling of cores, the Fourier transform in time was used. The time step is $\tau=5$ ps, the spatial step is $h=250$ μm. The relative difference in refractive indices δn_j changes with a characteristic length $L_{\mathrm{ref}}=1$ mm, the intermediate values $\delta n_j(z)$ are determined by a spline.

In order to describe the experimentally observed beam stirring, the parameters of the coupling strength J and the maximum variation of the refractive index $\delta n_{\max}$ were varied. First of all, the simulation results showed that the beam stirring among the cores is observed only in the case of relatively weak coupling $J<\delta n_{\max}$, while for strong coupling a non-trivial intensity distribution across the supermodes is observed. For each experimental power, about 150 simulations were carried out with parameters varying in the reasonable range $\delta n_{\max}\in[10^{-6},10^{-4}]$ and $J\in[10^{-7},10^{-5}]$. The most suitable parameters for describing the experimental results were chosen ($\delta n_{\max}=3\times10^{-6}$ and $J=9\times10^{-7}$ for which the numerical simulation agrees well with the experimental data for output power difference in the cores as a function of input peak power (see Fig. 2(b)). The main difference of the simulated curve is the presence of short-scale fluctuations which are not pronounced in the experimental data consisting of separated points.

Simulation with the same parameters of the longitudinal power variations in the individual cores at maximum input power $P_{\mathrm{in}}=6.32$ kW is shown Fig. 5(b). The input power injected in the central core starts oscillating between the fiber cores with ~100% relative variations at the initial part of the MCF. After 3–5 m the oscillations amplitude is greatly reduced whereas the average powers tend to equi-partition reached at $\sim$ 10 m amounting to ~14% in each core with fluctuations of <5%) that agrees well with the experimental data (Fig. 3). It's important to note that the power equipartition in the cores occurs not simply in the case of weak coupling ($\delta n_{\max}/J=3.3$ for the best-fit data), but also depends on absolute values. For example, if we increase the coupling strength J and refractive index variation $\delta n_{\max}$ by an order of magnitude, we observed chaotic power oscillations in the cores with no change in their amplitudes with

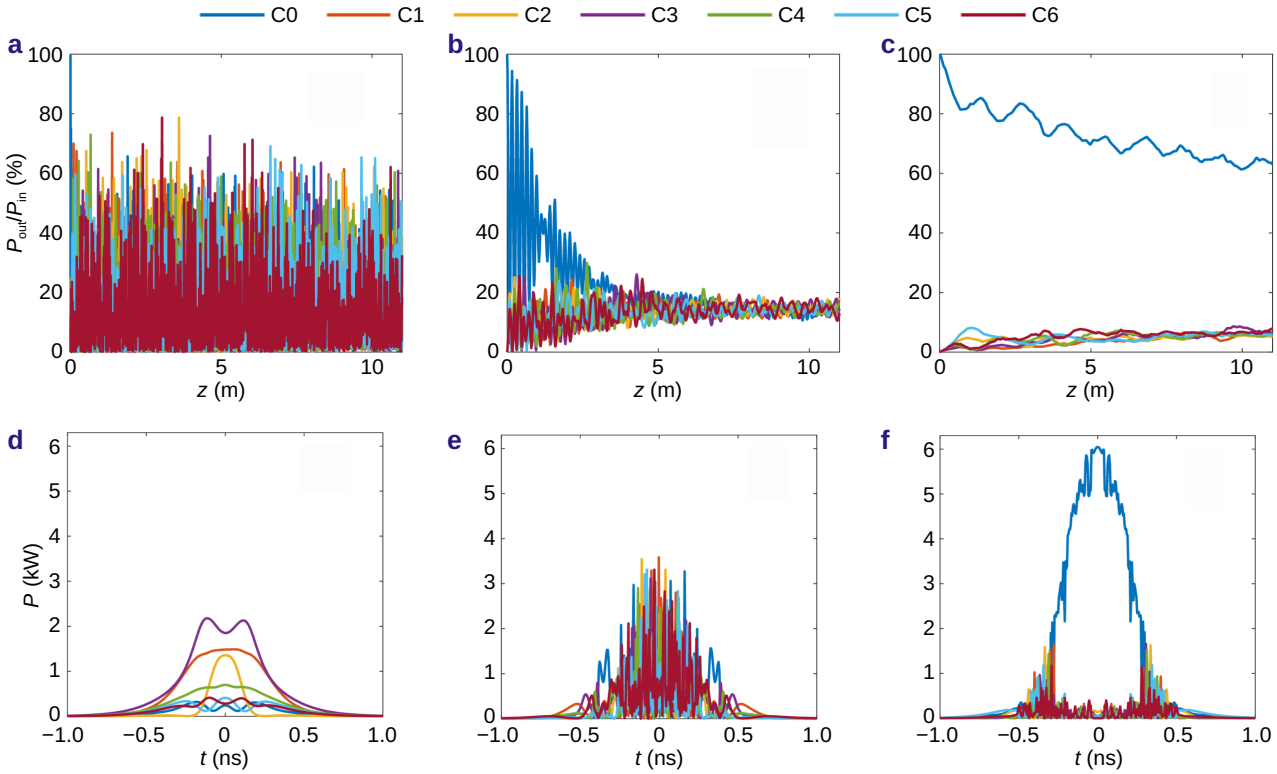


Fig. 5 | The power distribution along the fiber in different cores normalized to input power P_{in}=6.32 kW and corresponding output pulses at MCF parameters: (a, d) $\delta n_{max}=3\times10^{-5}$, $J=9\times10^{-6}$; (b, e) $\delta n_{max}=3\times10^{-6}$, $J=9\times10^{-7}$;(c, f) $\delta n_{max}=3\times10^{-6}$, $J=10^{-7}$.

distance along the fiber (see Fig. 5(a)). In this case, the shape of the pulse in the cores is slightly deformed, since the nonlinear phase is disrupted due to a large change in the refractive index resulting in predominantly linear (randomly varying) redistribution of the whole pulse (see Fig. 5(d)). Besides, a decrease in coupling strength with experimental refractive index variation prevents linear interaction between the cores, and the equi-partition effect disappears (Fig. 5(c, f)) with the pulse predominantly propagating in the central core.

In the case of optimal values of the refractive index variation δn_{max} and the coupling strength J, the effective length of energy transfer between the cores at high peak power turns out to be greater than the nonlinear length $L_{NL}=1/(\gamma P_{in}/7)$. A large nonlinear phase shift leads to the emergence of statistically independent sub-pulses in the individual pulse, which lead to the occurrence of oscillations (see Fig. 5(e)), and sub-pulse number $N=\sqrt{1+(\gamma P_{in}z/7)^2}$ is determined by the nonlinear phase incursion in each core in average. So, after averaging over pulse length the power fluctuations in the cores are reduced by a factor of $\sqrt{N}$, and their magnitude depends on the input power and the distance according to the following law:

$$\frac{\Delta P(z,P_{in})}{P_{in}}=\frac{\Delta P(z=0)}{P_{in}}\left(1+((\gamma P_{in}z)/7)^2\right)^{-1/4}. \quad (2)$$

This analytical approach is in good agreement with the experimental and numerical data for the dependence on both the pulse peak power (Fig. 2(b)) and on the propagation distance (Fig. 3) taking into account that it is applicable for relatively long distances. Thus, the beam stirring effect may be interpreted as a statistical process resulting from weak random coupling combined with nonlinear phase accumulation. In this scenario, nonlinear phase shifts modify the direction of energy transfer between cores, leading to a diffusive spatial redistribution of power, that also leads to fluctuations of instant power along the pulse in individual cores. So, such evolution may be treated as spatiotemporal beam stirring of individual pulse.

In addition to the equi-partition between the cores, the statistical averaging over N sub-pulses may also be a reason of the bell-shaped beam formation at high peak power (Fig. 4(c, f, i)), in contrast to the speckled structure observed at low power (Fig. 4(a, d, g)) when the whole pulse is randomly distributed between the cores with the subsequent interference of partial beams in far field.

4 Results and discussion

So, the effect of beam stirring between the weakly coupled cores of multicore fiber experimentally observed for sub-nanosecond narrowband pulses of several kW peak power

propagating in 11-m long 7-core fiber appears to be a new nonlinear effect. In contrast to low-power domain where the output power distribution in the cores is random with large fluctuations sensitive to fiber disturbances, at high power of the input pulse injected in the central (or another) core the output power becomes equalized between the cores with fluctuations reduced to <5% being insensitive to disturbances. Similar behavior is observed in cut-back experiments showing that at short propagation distances even high-power pulse is randomly distributed between the cores approaching equi-partition with increasing distance. At the same time, the output beam with equalized core powers measured in a far field tends to a stable bell-shaped profile, in contrast to strongly speckled unstable beam observed at low powers.

Based on the performed numerical modeling and analytical treatment, the observed nonlinear beam stirring effect has a statistical nature. At low peak power, a weak optical coupling of the core modes in the presence of random refractive index variations results in random redistribution between the cores of the pulse as a whole, with fluctuations of power difference in the cores of the order of their average values. At high peak power, the nonlinear phase shift with increasing propagation distance becomes large (being inconstant along the pulse) thus changing the direction of power conversion between the cores. As a result, the power starts oscillating along the pulse in all cores; according to an analytical estimate, sub-pulses number reaches $N \sim 100$ in our experiment. Though within each ~ 10-ps sub-pulse the power distribution between the cores is random, averaging in time domain over the whole pulse results in reduction of fluctuations by a factor of $\sqrt{N}$, so the power distribution is equalized and stabilized (see the video file "Pulse evolution" in the supplementary information). Similar averaging of different speckled patterns in spatial domain arising from interference of partial beams within the sub-pulses leads to the formation of a bell-shaped stable beam in a far field.

In its external manifestations, the observed spatiotemporal beam stirring effect in MCF looks similar to the Kerr beam self-cleaning (BSC) revealed earlier in multimode fiber (MMF) at nearly the same pulse parameters and fiber length[15]. As it was shown later[16,17], the BSC effect may be described by statistical mechanics. At low peak powers of a pulse propagating in a graded-index MMF (experiencing random mode coupling due to bending etc.) the distribution of transverse modes tends to random one with nearly equal average values resulting in a highly speckled output beam. At several kW-level peak power when the nonlinear (Kerr) four-wave mixing of modes comes into play, the output beam takes a smooth bell-like shape with mode distribution over their quantum number approaching the Rayleigh-Jeans law (RJ) with dominating fundamental mode and decreasing number of higher orders[17] that corresponds to thermodynamic equilibrium at low temperature. In the case of strongly coupled cores of multicore arrangements[14] similar low-temperature RJ distribution may be observed but for supermodes, so that the power distribution between cores is not equalized. So, in spite of some similarity the results presented here significantly differ from previous ones[14–17]. One of the possible explanations of equi-partition in frames of RJ distribution may be associated with a temperature tending to infinity, but in MCF it is rather related to supermodes with different propagation constants. It seems more relevant in our case to treat core modes basis since supermodes may not be formed at weak nonlinear coupling in the presence of random linear coupling. So, we have individual core modes which are degenerate due to nearly equal properties of the cores in hexagonal MCF. It should be noted that in the case of degeneracy the RJ distribution may be reduced to equi-partition even at low temperature.

Thus, the detailed analysis has shown that the equalization effect may be interpreted as a statistical process resulting from weak random coupling combined with nonlinear phase accumulation. In this case, nonlinear phase shifts modify the direction of energy transfer between cores so that the pulse envelope becomes modulated and the spatial redistribution of the multiple sub-pulses is statistically averaged. As a result of such spatio-temporal beam stirring, the core powers are equilzed but with greatly reduced fluctuations, in contrast to pure linear random coupling of the pulse as a whole with 100% power fluctuations in each core. The insensitivity to disturbances and robustness of the beam stirring effect observed at several kW peak powers is a statistical result and the source of statistics is clear – large nonlinear phase shift leading to variable power conversion between cores in spatial domain and formation of large number of sub-pulses in temporal domain which are statistically averaged along the pulse. So, in the case of spatiotemporal beam stirring the statistical approach is applicable to a single pulse (as well as to pulse trains). Though the reason of statistical behaviour is not discussed in detail for the BSC effect in MMF (see ref.[16,17] and citation therein), large nonlinear phase shift may play a similar role there.

5 Conclusions

In conclusion, the novel effect of spatiotemporal beam stirring is quite important for the fundamental research and development of nonlinear photonics in multimode and multicore fibers, paving the way for new technologies and their practical applications. In particular, it may be applied for power-equalized light amplification in the weakly coupled cores of active MCFs to extremely high powers. The effect of beam quality improvement in far field is also interesting for applications such as high-power beam combining[9] and nonlinear imaging[18], but it requires further exploring the details, namely phase properties of the partial beams and combined beam, which define coherent or incoherent regime. For the sake of knowledge completeness and future

developments it is also interesting to investigate the effect for MCFs of various topologies and high-peak-power pulses of various length and spectrum.

References

1. Richardson DJ, Fini JM, Nelson LE. Space-division multiplexing in optical fibres. *Nat Photonics* **7**, 354–362 (2013).
2. Rademacher G, Puttnam BJ, Luís RS et al. 10.66 Peta-Bit/s transmission over a 38-core-three-mode fiber. In *2020 Optical Fiber Communications Conference and Exhibition (OFC)* 1–3 (IEEE, 2020).
3. Michaille L, Bennett CR, Taylor DM et al. Multicore photonic crystal fiber lasers for high power/energy applications. *IEEE J Sel Top Quant Electron* **15**, 328–336 (2009).
4. Zhao ZY, Tang M, Lu C. Distributed multicore fiber sensors. *Opto-Electron Adv* **3**, 190024 (2020).
5. Wolf A, Dostovalov A, Bronnikov K et al. Advances in femtosecond laser direct writing of fiber Bragg gratings in multicore fibers: technology, sensor and laser applications. *Opto-Electron Adv* **5**, 210055 (2022).
6. Kuznetsov AG, Wolf AA, Egorova ON et al. Spectrum collapse in a 7-core Yb-doped fiber laser with an array of fs-inscribed fiber Bragg gratings. *Opt Lett* **48**, 3603–3606 (2023).
7. Alon Y, Halstuch A, Sidharthan R et al. Femtosecond Bragg grating inscription in an Yb-doped large-mode-area multicore fiber for high-power laser applications. *Opt Lett* **45**, 4563–4566 (2020).
8. Klenke A, Jauregui C, Steinkopff A et al. High-power multicore fiber laser systems. *Prog Quant Electron* **84**, 100412 (2022).
9. Klenke A, Müller M, Stark H et al. Coherent beam combination of ultrafast fiber lasers. *IEEE J Sel Top Quant Electron* **24**, 0902709 (2018).
10. Andrianov AV, Kalinin NA, Anashkina EA et al. Selective excitation and amplification of peak-power-scalable out-of-phase supermode in Yb-doped multicore fiber. *J Light Technol* **38**, 2464–2470 (2020).
11. Balakin AA, Skobelev SA, Andrianov AV et al. Coherent amplification of high-power laser radiation in multicore fibers from a rectangular array of cores. *Opt Lett* **46**, 246–249 (2021).
12. Chekhovskoy IS, Rubenchik AM, Shtyrina OV et al. Nonlinear combining and compression in multicore fibers. *Phys Rev A* **94**, 043848 (2016).
13. Andrianov AV, Kalinin NA, Koptev MY et al. High-energy femtosecond pulse shaping, compression, and contrast enhancement using multicore fiber. *Opt Lett* **44**, 303–306 (2019).
14. Kirsch MS, Pyrialakos GG, Altenkirch R et al. Observation of Joule-Thomson photon-gas expansion. *Nat Phys* **21**, 214–220 (2025).
15. Krupa K, Tonello A, Shalaby BM et al. Spatial beam self-cleaning in multimode fibres. *Nat Photonics* **11**, 237–241 (2017).
16. Wu FO, Hassan AU, Christodoulides DN. Thermodynamic theory of highly multimoded nonlinear optical systems. *Nat Photonics* **13**, 776–782 (2019).
17. Mangini F, Gervaziev M, Ferraro M et al. Statistical mechanics of beam self-cleaning in GRIN multimode optical fibers. *Opt Express* **30**, 10850–10865 (2022).
18. Feng HG, Chen X, Zhu RZ et al. Seeing at a distance with multicore fibers. *Opto-Electron Adv* **7**, 230202 (2024).

Acknowledgements

The work is supported by the Russian Science Foundation (grant 21-72-30024-П) and the work of A.Yu.Kolesnikova on simulation – by the Ministry of Science and Higher Education of the Russian Federation (FSUS-2025-0010).

Author contributions

A.Y.K. made the numerical model and performed the simulation. M.D.G. and N.B. assembled the experimental setup and performed the measurements. E.V.P. derived the model and performed the analytical calculations. D.S.K. supervised the experimental part of the project. S.A.B. proposed the original idea and supervised the project. All authors wrote the paper.

Competing interests

The authors declare no competing financial interests.

Supplementary information

Supplementary information for this paper is available at
https://doi.org/10.29026/oea.2026.260036

Open Access This article is licensed under a Creative Commons Attribution 4.0 International License, which permits use, sharing, adaptation, distribution and reproduction in any medium or format, as long as you give appropriate credit to the original author(s) and the source, provide a link to the Creative Commons license, and indicate if changes were made. To view a copy of this license, visit http://creativecommons.org/licenses/by/4.0/
©The Author(s) 2026.

Published by Editorial Office of *Opto-Electronic Advance*, Institute of Optics and Electronics, Chinese Academy of Sciences.

Opto-Electronic Journals Group
www.oejournal.org

Scan for Article PDF